American Scientific Research Journal for Engineering, Technology, and Sciences (ASRJETS)
ISSN (Print) 2313-4410, ISSN (Online) 2313-4402

http://asrjetsjournal.org/

Geochemical Characterisation of Anatexite within High Grade Migmatite Complex Terrain from Ogbomoso, Southwest of the Nigerian Precambrian Basement Complex

Adegoke Olukayode Afolabi[a]*, Rukayat Omobolanle Lawal[b], Esther Olufunmilayo Ogunmiyide[c], Kolade Adeosun[d]

[a,b,c,d]*Department of Earth Sciences, Ladoke Akintola University of Technology, Ogbomoso, 210214, Nigeria*
[a]*Email: oaafolabi@lautech.edu.ng*
[b]*Email: ruksan001@yahoo.com*
[c]*Email: ogunmuyideesther@yahoo.com*
[d]*Email: adeosunkolade1@gmail.com*

Abstract

Migmatite rocks are complex rocks largely due to the degree of partial melting and nature of parent rocks of this rock type. Partial melting or anatexis yield metatexite and diatexite components with variable mineralogical and chemical compositions. The nature of fractionation of elements during anatexis is not clearly understood. The migmatite quartzite gneiss complex of southwestern Nigeria exposed at Ogbomoso was studied in order to constrain the geochemical character of its metatexite and diatexite components. Field mapping revealed migmatite with stromatic, surreitic and dictyonitic structures represented the metatexite while parts of the migmatite with schollen structure and granitic component represent the diatexite. Several sections of representative samples were cut and examined for mineralogical compositions. Thin section analysis revealed occurrence of hornblende and garnet with plagioclase, microcline, biotite and muscovite implying greenschist to amphibolite facies for the migmatite quartzite gneiss complex. Twelve representative samples were selected and analysed for their elemental concentrations using the Inductively Coupled Plasma Mass Spectrometry (ICP-MS).

---

* Corresponding author

Major oxide geochemical data revealed a silica enriched migmatite with schollen structure having moderate alkali concentration while the granitic component and porphyroblastic gneiss with lesser silica concentrations showed relative Na_2O and K_2O enrichments respectively. Classification plots demonstrated that the migmatite of the study are ortho gneisses and have a Tonalite Trondjhemite Granodiorite (TTG) parentage. Trace element ratios revealed that the diatexite had lower than average upper continental crustal values for Nb/Ta ratio while the metatexite revealed average values slightly above 12. Normalised REE plot discriminated the migmatite with schollen structure as parts having HREEs closest to chondrite values.

Keywords: Migmatite; Metatexite; Datexite; Anatexis; Geochemical-data.

1. Introduction

The complexity and variability in the mineralogical and chemical compositions of migmatite in Nigeria is a major influence in its exploitation. Understanding the mineralogy and geochemistry of migmatite components is therefore crucial. Migmatites are a complex group of rocks due to the variation of rock types intermingled into one complex terrain. This rock hosts granitic, granodioritic and amphibolite components. Granitic components in migmatites have been, where exposed, used as quarries for granite; road construction; granite slabs. The migmatite gneiss quartzite complex covers about 50% of the Precambrian Basement complex. Also, groundwater extraction from weathered to freshly weathered basement rocks, mainly from the migmatite gneiss quartzite complex, is extensive and intensive and this has major effect on the groundwater chemistry, especially hardness variability. The competence, nature and chemistry of the components of the migmatite are based on the amount and type of feldspar content. Feldspars, under hydrous conditions, are susceptible to degradation into clay deposits. The migmatite of southwestern Nigeria hosts granitoids of varied mineralogical and chemical composition with equally varied geotechnic and geochemical properties. The nature and mineralogy of migmatite gneiss complex of the Precambrian Basement Complex of Nigeria, the oldest member of the crystalline basement has been shown to be composed dominantly of i) Early gneiss, ii) Amphibolite and iii) Granitic components [1]. Migmatites, in their evolution, are genetically related to granitisation, anatectic granites [2]. Granite exposures in the migmatite gneiss complex underlying some parts of the southwestern part of the Nigerian Precambrian Basement Complex are impressive and extensive. The granite component within the migmatite gneiss complex underlying Ogbomoso, southwest Nigeria, do not show more than compositional borders with the migmatite, the banded gneiss and the quartzite. Other varieties with granitic composition include the porphyroblastic granitic gneiss. The mineralogy of granitic rocks, as observed from field evidences, describes rocks from quartz dioritic to true granitic compositions [3] with fabric and micro-textures emphasising magmatic origin. Experimental and petrographic evidences of [4] showed that rocks of granitic compositions are probable products of thermal minima on the liquidus lines in both Ab-Or-Q and Ab-An-Or-Q systems. Both systems are analogous to felsic magma composition. Felsic magma is believed to be the primary source of these rock varieties. The production of this felsic magma during anatexis may be ascribed as the unequivocal process by which granitic components are incorporated in many crystalline migmatite terrains. Two magmatic models evoked to explain granite formations are i) crystal fractionation of mafic magma and ii) partial melting of pre-existing crustal rocks (realm of metasomatism). Experiments on partial melting reveal that proportions of melt are dependent on protolith and temperature-pressure conditions [5,6]. Low degrees of partial melting produce

felsic melts of granitic composition that start to collect along grain boundaries and microfractures. This melt separates to form discrete leucosomes. Melt and solid fraction of this nature produce metatexite migmatite. Increased temperatures above melt escape threshold favour higher degrees of partial melting that enhance dilute bulk flow or magma flow [5] with suspended crystals. This melt, destroying pre-existing structures, form diatexite migmatite. Reference [7] showed that a high degree of partial melting of Tonalitic-Trondhjemitic-Granodioritic crust is capable of producing diatexite. Migmatite complex covers about half of the total land covered by the Precambrian Basement Complex of Nigeria. The southwestern part of this complex is almost covered by this basement complex except for the Dahomey basin (Fig. 1a) located at the coastal area. Extensive migmatization from regional metamorphism of the polyclic Precambrian Basement complex is a prominent geologic process that dominated more than nine over ten of the life span of the Earth. Anatexis is a major geologic process, during migmatization, responsible for the characterisation of the many types of migmatites [8]. The nature and chemical character of the anatexite underlying Ogbomoso, southwestern part of the Nigerian Precambrian Basement complex, is examined in order to understand possible ionic diffusion that accompanied metasomatic reactions during anatexis that defined the variation in mineralogy.

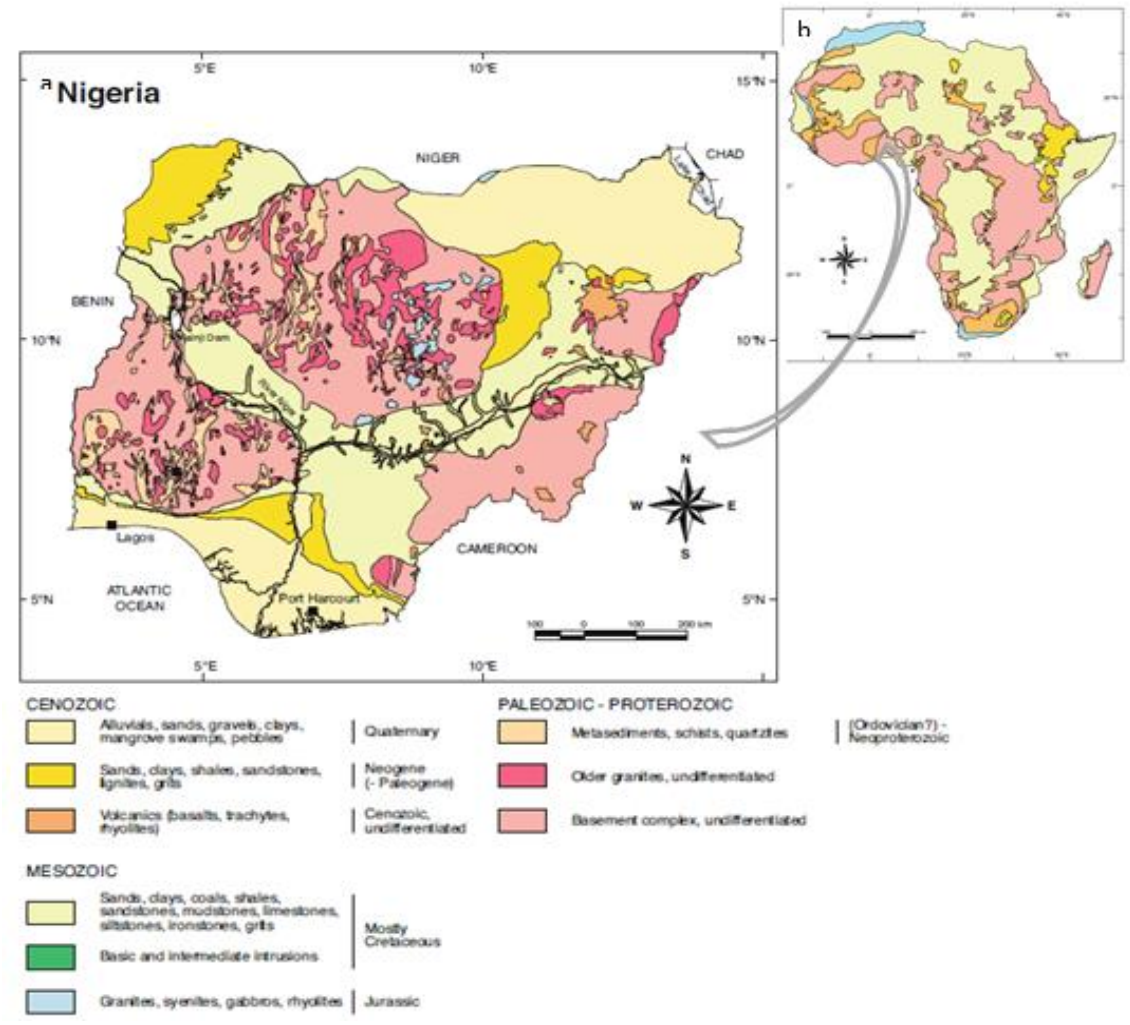

Figure 1: Simplified geology of Africa (a) after [12] and (b) Nigeria after [13].

2. Geological Setting of the Migmatite

Migmatite gneiss complex of Nigeria is the oldest member of the Precambrian basement complex [9,10] and therefore has suffered multiple episodes of deformation, metamorphism, metasomatism, uplift and folding. The dominant rock type in the southwestern part of the Nigerian Basement complex is the wide spread migmatite gneiss complex that is closely associated with quartzite bodies with evidences for uplift. Reference [10] grouped these two litho-structural units as the oldest member of the Nigerian Precambrian Basement complex. In the Ogbomoso area the gneiss complex covers more than 60% of the lithologic units underlying the area. Reference [11] gave an account of the geology of the area. In the southwest of the Nigerian Precambrian Basement complex (Fig. 1a and b) [12,13], migmatite exposures occurred closely with ridges of quartzite/quartz schist (Fig.2b). The migmatite occurs mostly as lowlying bodies that conform to the topography. Occasionally they may rise to 50 - 100 meters above the ground level and displaying dome to turtle back plutons. In Ogbomoso, exposures of migmatite at Ikoyi, Iresa, Iwo-Ile areas displayed structures characteristic of schollen – Dictyonite (phlebitis) – stromatite - surreitic (Figs. 3 and 4). These structures qualify the migmatite terrain in Nigeria as polymigmatitic complex. The pattern of distribution of these structures that describe migmatite is yet to be studied and is not the scope of this study. The description of migmatite is based on two or three components [8]. On the bases of two components, migmatites are described based on paleosome (i.e. unaltered or slightly altered protolith) and neosome (i.e. newly produced crystallised melt from partial melting). The paleosome is also known as mesosome while the neosome is subdivided into leucosome (leucocratic part having granitic composition) and melanosome (the melanocratic part rich in mafic minerals such as dark micas, amphibole).
The nomenclature and complexity of migmatite is based on the nature and processes of formation of the neosome and its relationship with the paleosome. The understanding of migmatite is dependent of the study of each of these components as closed systems. Agmatitic and schollen migmatite are striking characteristic structures of migmatite that describe anatexis. In the migmatite complex of the study, schollen migmatite (Fig. 3a) was observed and usually at locations distal to the quartzite exposures. Melanocratic residuum of amphibolitic protoliths (paleosome) forming rafts with fairly rounded edges is dissected by veins of felsic compositions (neosome) to form schollen migmatite. Figure 3b showed granitic component formed from several streams of leucocratic veins. Field evidences revealed that stromatic migmatite are localised close to the occurrences of quartzite exposures. Extensive linear leucosomes are observed to form parallel to near parallel bands that are separated by greyish paleosome (mesosome). Migmatite of stromatic structures (Fig. 4a and b) occurring in Ogbomoso area were observed in Iresa-Apa, General area, Iwo-Ile. All occurrences were in close proximity to quartzite/quartz schist outcrops. In these exposures leucosome bands consisted of quartz, alkali feldspar and minor amounts of muscovite. Bands vary in thickness from 0.15cm to 10cm and occasionally reached 2ft. When they reach 2ft in width they usually formed pegmatitic/quartzofeldspathic veins. The infiltration and lack of very dark components may presuppose injection of granitic fluid (Fig. 4a and b). [11] mapped this migmatite type as banded gneiss while [10] described them as grey gneisses. The nature of injection may either be externally/open system (external migmatization is, for example, responsible for the formation of phlebite) or internally/closed sytem (internal migmatization forming e.g. venite) [8].

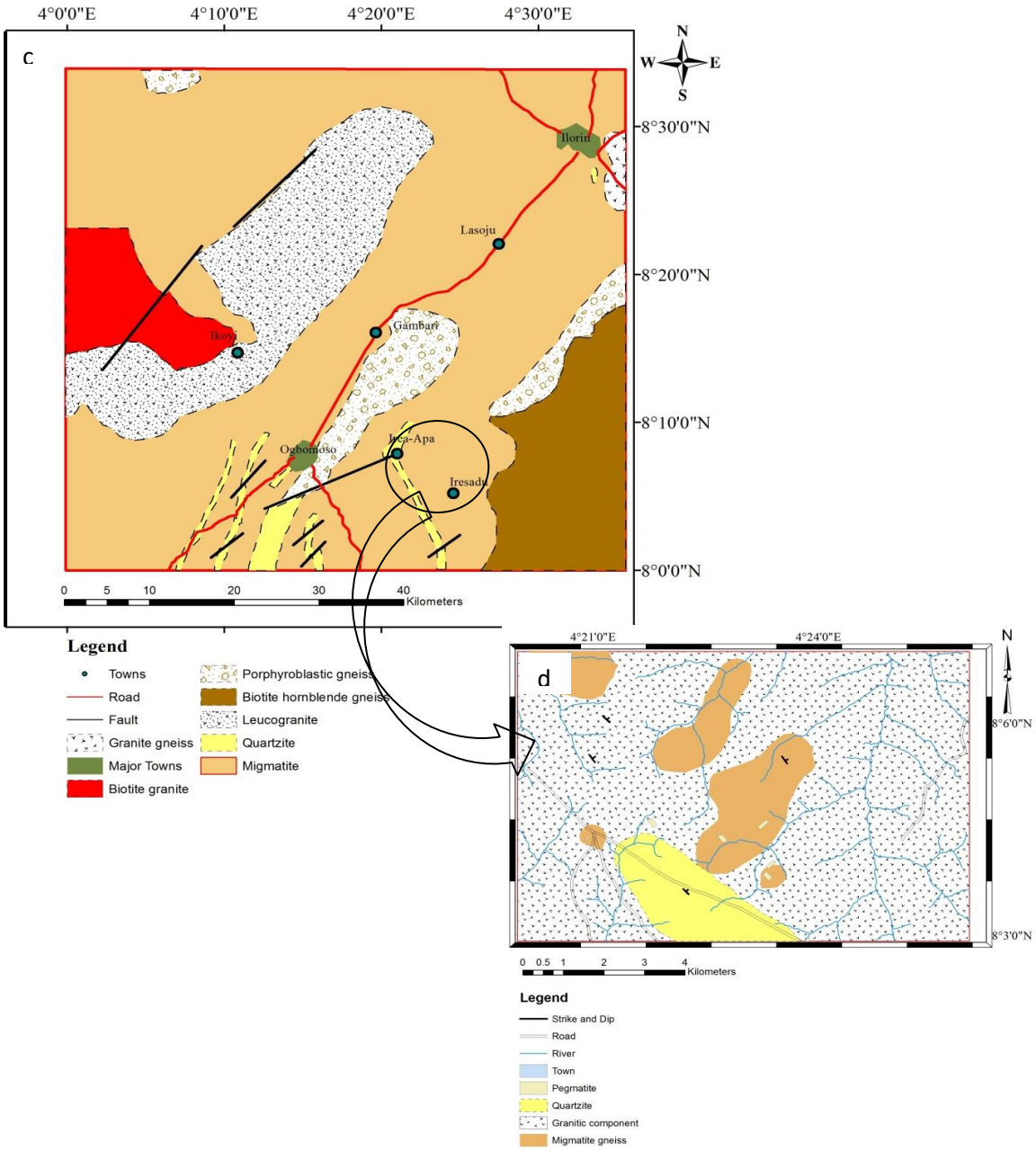

Figure 2: Geological map of the study.

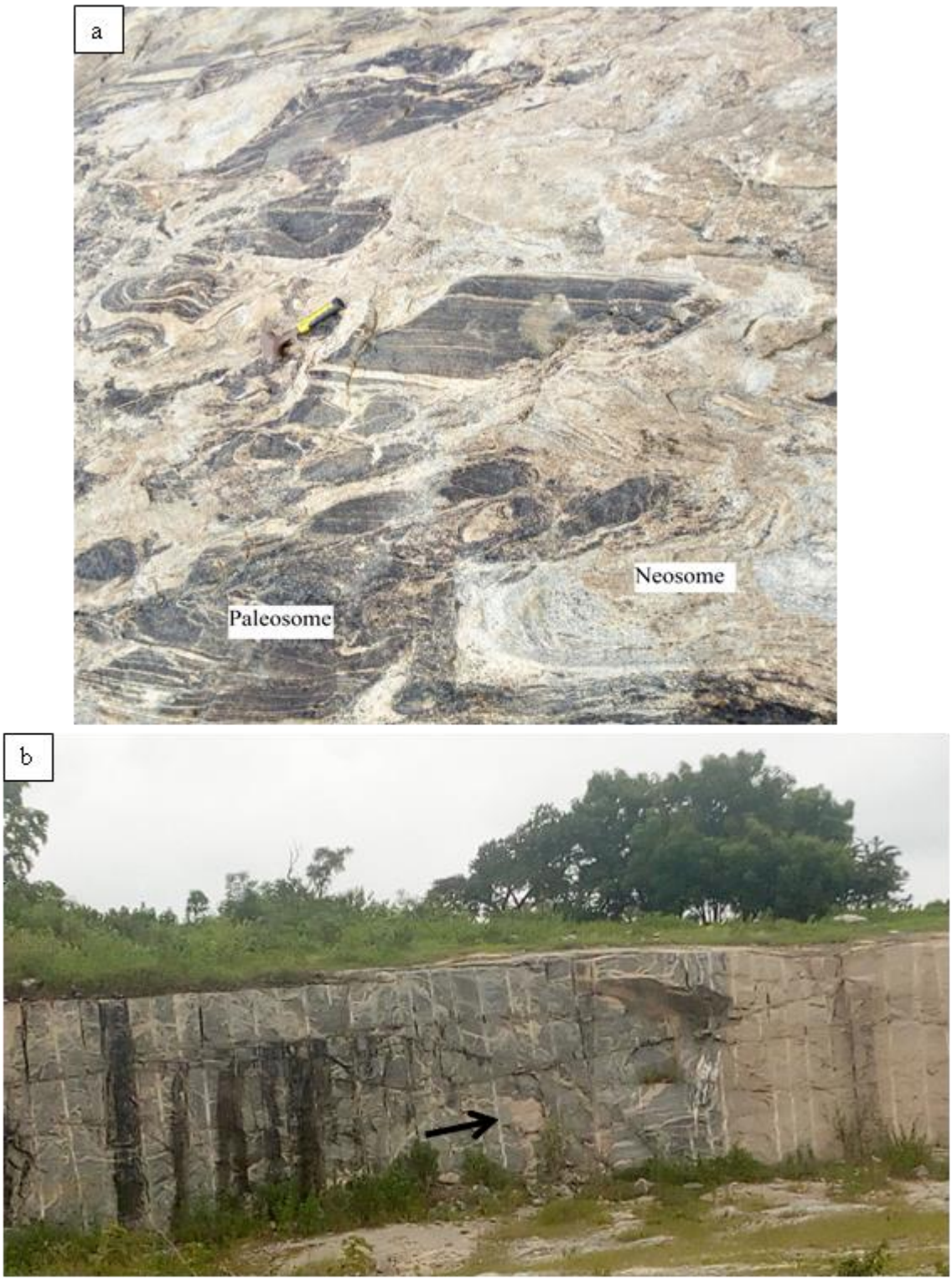

Figure 3: a) Schollen structure in migmatite revealed rafted fragments of dark mafic protoliths describing the Paleosome having sharp boundaries with the more felsic neosome parts. Felsic components also form selvedge. b) Migmatite and granite form compositional boundary. Veins of leucosome pond granitic fluid to form enclaves of granite within the migmatite (arrow).

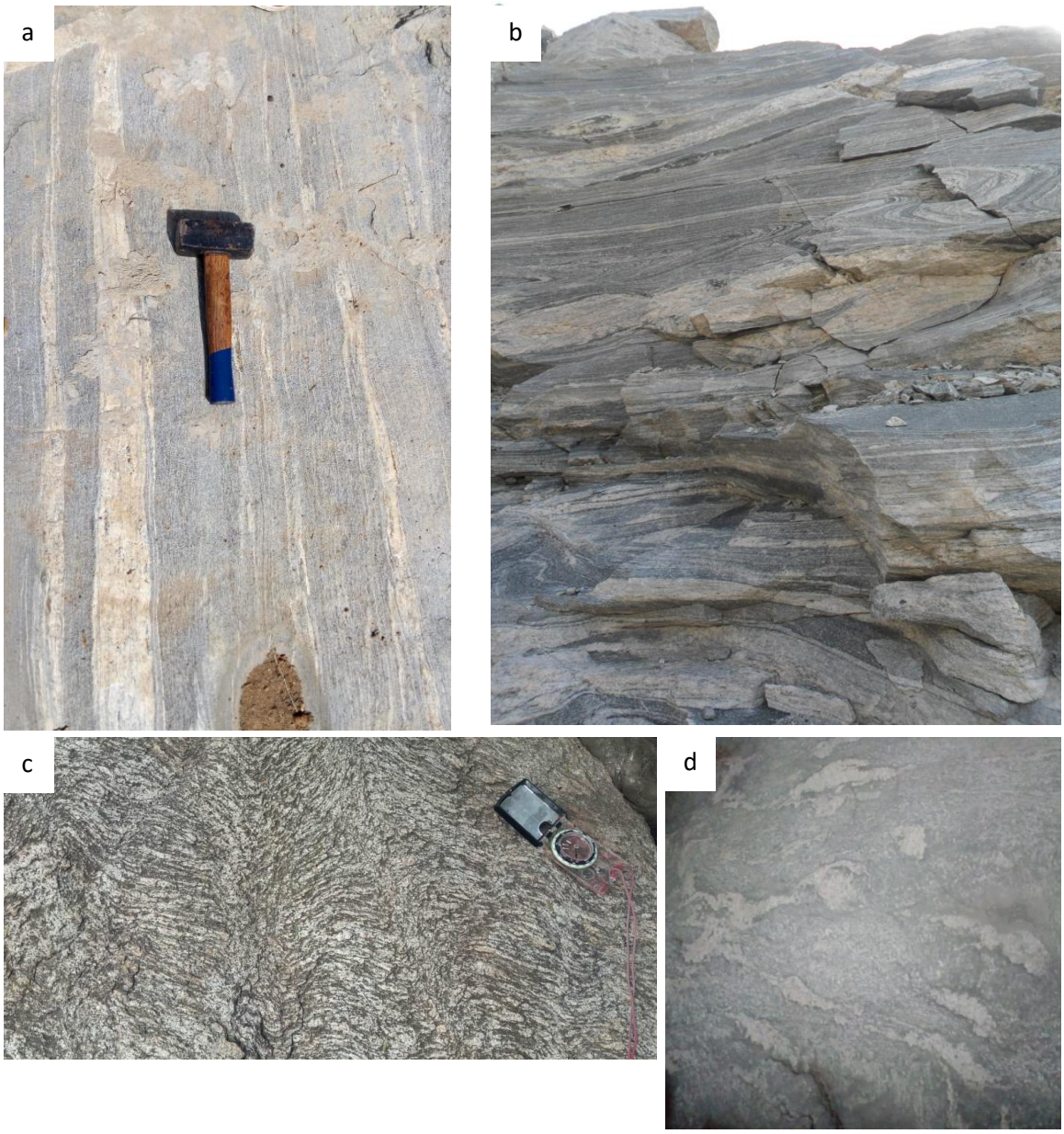

Figure 4: a) Stromatic migmatite gneiss, at Iresa-Adu, with leucosome bands of different widths running through greyish mesosome. b) Perceived injected granitic fluid forms foliation in migmatite at Iresa-Apa. c) Veins of leucosome form net-like structure display crenulation suggesting deformation. d) Ponding of patches of leucosome describes surreitic structure.

An exposure found at Takie-Ikoyi enroute Igbeti in Ogbomoso showed that dictyonite/phlebite exposures (Fig. 4c) occurred as localised portion within expanse of schollen migmatite. Stromatic gneiss exposed at General – Stadium area separated the quartzite from the dictyonite. Dictyonite have been described as porphyroblastic [14] gneiss with thin or net-like leucosome bands appear as characteristic foliation (S_1) with evidence for crenulation (S_2) (Fig. 4c). The leucosome are rich in quartz and feldspars while the melanosome show enrichment in biotite associated with feldspars and quartz in lesser amounts.

Reference [15] described almandine-amphibolite facies for the 'Older Granite' orogeny that deformed and metamorphosed majority of the rocks of the basement complex of southwestern Nigeria. The mineral assemblage for this facies includes reddish-brown biotite, bluish hornblende, magnetite with sphene rims and relict pyroxene. Garnet, biotite, hornblende and plagioclase (Fig. 5) describe upper amphibolite facies for the migmatite of the study.

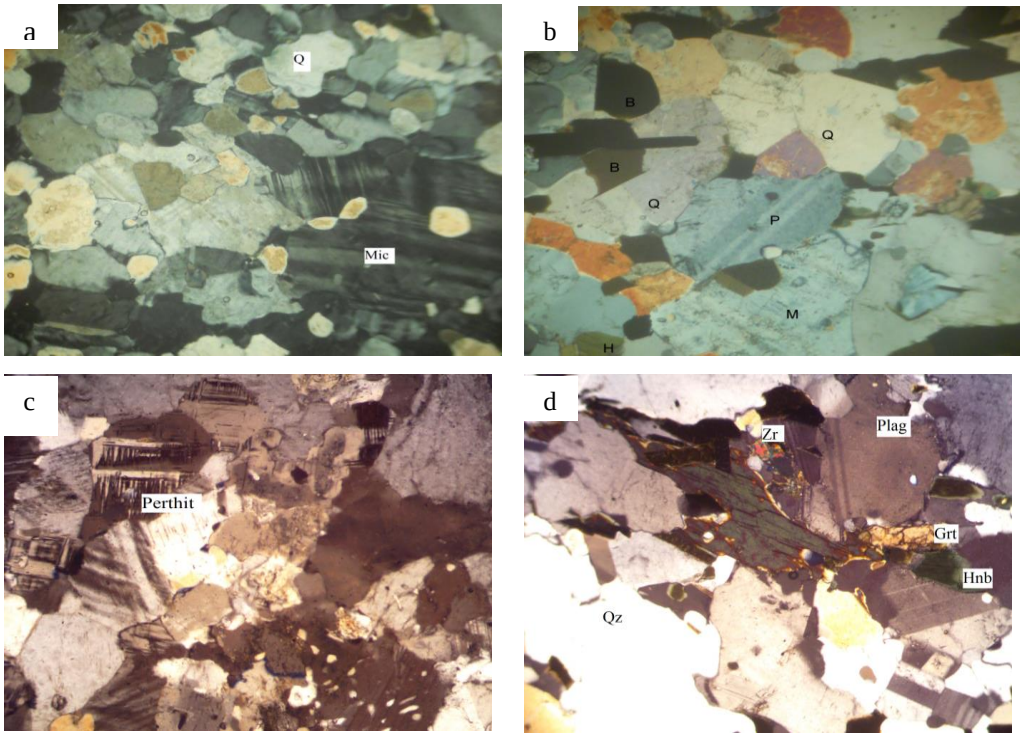

Figure 5: a) Migmatite mineralogy revealed quartz (Q) biotite (B) and microcline (Mic) in (a) and orthoclase and lesser amount of plagioclase in (b). c) Perthites preponderance was observed in the porphyroblastic gneiss. d) the granitic component has quartz (Q), biotite (B), hornblende (H), more plagioclase (P) and less alkali feldspar. Garnet (Grt) crystals and zircon (Zr) occur as accessory minerals in samples cut from the granitic component.

Variation in metamorphic grade attributed to level of emplacement rather than time may not be entirely true. The first order classification of anatexite into metatexite and diatexite [16] (Fig. 6) based on i) nature of protolith, ii) rate of cooling, iii) intensity of partial melting and iv) deformation may give better understanding to the variation in metamorphic grades. Variation in metamorphic grade may well be linked to all four factors listed above. Field study revealed occurrences of stromatic gneiss, a metatexite, are closely associated with quartzite and grade into dictyonite/phlebite and further away are occurrences of schollen structures.

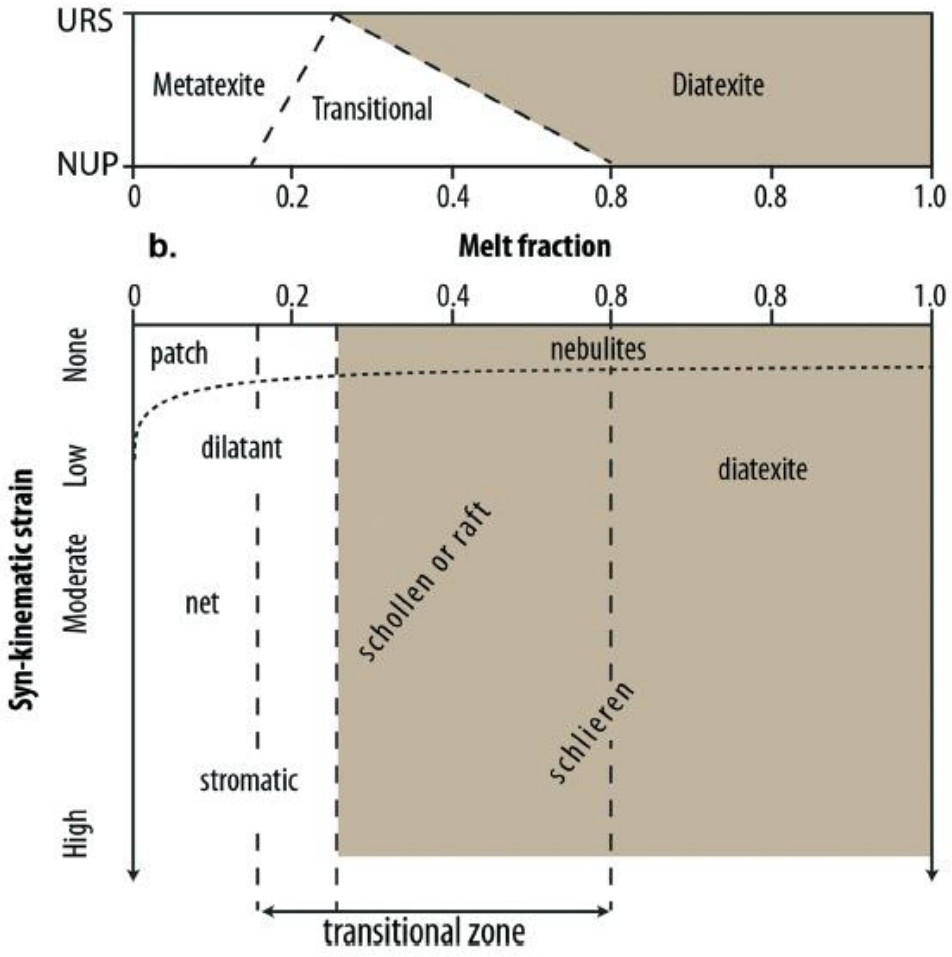

Figure 6: First and second order classification for migmatite [after 16].

3. Materials and Methods

Field mapping exercise done during the dry season, January – March, facilitated the constraining of the parts and structures of the migmatite quartzite gneiss complex underlying the study. Samples were obtained mostly from freshly exposed outcrops at quarry sites. Several thin sections of parts of the migmatite complex were cut at the University of Ibadan, Ibadan. Mineralogical compositions were viewed at Ladoke Akintola University of Technology, Ogbomoso under a petrographical microscope. Photomicrographs of selected views from sections were taken using a x5mm AmScope® camera. From the fresh samples obtained, twelve samples from the migmatite complex representing parts of the migmatite that correspond to the first order classification of migmatite given by [16] were pulverised and sent to ACME Laboratories at Vancouver, Canada for geochemical analysis to reveal elemental concentrations using Inductively Coupled Plasma Mass Spectrometry (ICP-MS). Plots from elemental concentrations obtained were created using GCDKit 4.1 and Petrograph 2beta softwares.

4. Results and Discussion

4.1 Major oxide and trace element geochemistry

Table 1 presents the major oxide concentration (wt.%) for the migmatite and its components and revealed siliceous compositions with average SiO_2 values of 65.66, 65.25 and 72.25 for granitic, porphyroblastic gneiss and migmatite components respectively. Average Al_2O_3 values are 15.65, 15.07 and 15.01 for the granitic, porphyroblastic gneiss and the migmatite components respectively. Alumina values showed more variability for the porphyroblastic gneiss as values correspond to both the least (13.50) and the maximum (16.84). SiO2/Al2O3 values showed a narrow range of values from 3.9 – 4.9 consistent with the partial melting processes argued for by [17]. Fe_2O_3 values for the migmatite showed the least concentration with values from 0.4 – 2.26 and average value of 1.25 while average Fe_2O_3 values for the granitic (5.02) and porphyroblastic gneiss (5.44) were similar.

Table 1: Major oxide and trace element geochemical data for the migmatite complex.

Sample Id	Gr1	Gr2	Gr3	OGB 01	OGB 02	OGB 03	OGB 04	OGB 05	Mgn1	Mgn2	Mgn3	Mgn4
SiO_2	64.99	66.37	65.61	66.47	61.06	65.13	64.44	69.16	71.4	73.18	71.7	72.71
Al_2O_3	16.58	15.52	14.85	14.73	13.50	16.84	15.70	14.59	15.02	14.84	15.21	14.96
Fe_2O_3	4.95	4.85	5.26	5.12	9.46	3.96	5.05	3.62	2.26	0.4	1.12	1.22
MgO	1.61	1.37	1.39	0.78	1.64	0.88	1.85	0.93	0.49	0.04	0.41	0.34
CaO	4.65	3.82	4.04	2.28	4.32	2.66	3.77	2.86	2.25	1.84	2.24	2.38
Na_2O	4.5	4.22	4.08	3.32	3.31	3.33	3.00	3.28	4.62	3.83	4.18	4.25
K_2O	1.61	2.15	2.25	5.29	2.94	5.76	4.51	4.33	2.9	4.58	3.89	3.03
TiO_2	0.49	0.68	1.03	0.64	1.70	0.44	0.42	0.40	0.29	0.03	0.16	0.16
MnO	0.07	0.08	0.08	0.07	0.19	0.06	0.08	0.08	0.03	0.005	0.02	0.01
P_2O_5	0.14	0.3	0.44	0.18	0.78	0.12	0.12	0.15	0.07	0.02	0.05	0.04
Ba	418	1336	1808	1833	1203	1307	1074	1176	681	1613	1261	1210
Co	32	9.4	11.9	7.0	17.4	8.1	12.2	8.7	26.4	25.6	20.3	31.2
Cs	1.9	1.1	0.6	1.4	3.0	1.2	3.8	2.6	2.5	2	1.5	0.8
Ga	18.8	21.2	19.6	21.2	22.0	17.7	16.9	16.5	18.3	15.6	16.4	15.8
Hf	4.2	7.5	11.6	8.9	13.6	5.3	5.4	4.9	4	1	2.8	2
Nb	4.8	19.3	22.2	21.6	30.0	15.6	9.9	10.6	5	0.6	2.8	2.4
Rb	53.8	70.9	47.8	160.6	168.3	180.8	156.7	112.6	109.9	89.7	79.9	57.2
Sn	1	2	2	3	11	2	5	21	0.5	0.5	0.5	0.5
Sr	427.9	582.8	686.1	356.8	339.2	456.3	399.1	303.7	343	489.6	476	538.2
Ta	0.6	3	3.1	1.1	1.8	1.0	1.0	1.0	0.6	0.2	0.5	0.5
Th	4.8	6.9	6.8	18.3	30.3	46.4	27.6	21.3	10.8	0.4	2.8	2.6
U	1.2	1.4	1.8	1.9	4.3	2.5	2.8	2.2	0.9	0.2	0.7	0.4
V	70	58	67	24	74	44	65	36	12	4	13	17
Zr	159.2	326	503.4	342.2	504.1	194.0	179.6	190.2	149.2	34.6	103.7	79
Y	8.9	26.6	41.3	28.3	58.5	19.8	25.5	34.8	3.9	0.5	3.6	2.2
Cu	12.6	3.7	8.4	14.1	22.9	30.7	15.9	9.6	0.7	0.4	3.3	3.7
Pb	0.9	0.9	1.3	7.1	13.6	7.4	6.9	8.2	1.6	2.6	3.4	2.6
Zn	47	61	63	84	153	49	49	46	62	6	27	27
Ni	13.4	7.8	8.1	3.1	13.9	10.6	11.0	5.6	2.1	0.2	4.4	2.4

Average CaO and MgO values showed a progressive increment from migmatite-porphyroblastic gneiss-granite. Mean CaO calculation from a range of 3.82 - 4.65 for the granitic component yielded 4.17 which represented the component with the highest lime content. Lime values ranged 2.28 – 4.32 and 1.84 – 2.24 for the

porphyroblastic gneiss and the migmatite respectively yielded corresponding average values of 3.18 and 2.18. For the magnesia average values for the granitic, porphyroblastic gneiss and migmatite components yielded 1.41, 1.22 and 0.32 respectively. Like Fe_2O_3 concentration (also herein treated as total FeOt) having similar average concentrations for the granitic and porphyroblastic gneiss components the TiO_2 and P_2O_5 average concentrations behaved in similar trend. Average TiO_2 concentration in the granitic (0.73) and porphyroblastic gneiss (0.72) was observed to be markedly higher than for the migmatite (0.16) components. Similarly average P_2O_5 values in the granitic (0.29) and porphyroblastic gneiss (0.27) were higher than for the migmatite (0.05). Alkali concentrations revealed more variable distribution pattern for the K_2O (std, 0.53) than Na_2O (std, 1.26). Potash values ranged from 1.61 – 5.76 while soda values ranged from 3.00 – 4.62. Plot of [18] illustrated the migmatite as ortho gneisses (Fig. 7). Classification plots adapted after [19,20] (Fig. 8a and b) revealed granitic to granodioritic compositions for the migmatite gneiss components of the study. The migmatite gneiss samples fell exclusively within the granite field while the products of metamorphic differentiation, the porphyroblastic gneiss fell in the granitic to dioritic field and granitic component samples fell in the granodioritic field. Normative feldspar plot after [21] revealed Trondhjemitic to granitic composition for the migmatite, tonalitic to granodioritic composition for the granite component and granodioritic to quartz monzonitic composition for the porphyroblastic gneiss (Fig. 8c). Plots of major oxide vs silica for the anatexite revealed negative correlation for all the oxides except for K_2O and Na_2O vs SiO_2 (Fig. 9). Bivariate scatter plots of K_2O and Na_2O vs SiO_2 revealing null correlation showed samples plotted to form discriminated fields (Fig. 10). Plot of CaO vs SiO_2 (Fig. 10) had samples from the granitic and porphyroblastic gneiss components plotted as negative correlation suggesting possible metamorphic differentiation along different lines with migmatite samples as source with higher silica values. Samples of the granitic components showed slight enrichment in lime concentrations supporting tonalitic compositions. Normative mineralogy also supports these compositions. Enrichment in CaO, MgO, Fe_2O_3, TiO_2 and P_2O_5 observed for the felsic melt responsible for the formation of granitic components is linked to anatectic melting. Alumina and alkali content appeared to be immobile. Average normative anorthite (An) values showed lowest for the migmatite (11) and highest for the granitic component (18). Granite and porphyroblastic gneiss (diatexite components) having dioritic compositions of variable degrees revealed norm diopside (Di) for samples Gr1 and OGB 04 respectively. For the diatexite components, higher normative values were observed for hypersthene (Hy), hematite (Hm), ilmenite (Il) and rutile (Ru). The aluminium saturation index (ASI) of [22] showed the anatexite components having metaluminous character while the migmatite revealed a peraluminous character (Fig. 11). Trace element concentrations reported in parts per million (ppm) (Table 1) showed variable patterns of mobility for large ion lithophiles (LIL). Porphyroblastic gneiss showed the highest average values in Ba (1318.60) and Rb (155.80). Average Ba (1187.33) and Rb (57.50) values for the granitic component were the lowest. This may be linked with feldspar compositions in the rock components. Average Ba and Rb concentration pattern was similar to K_2O concentration pattern. Strontium (Sr) concentrations were lowest

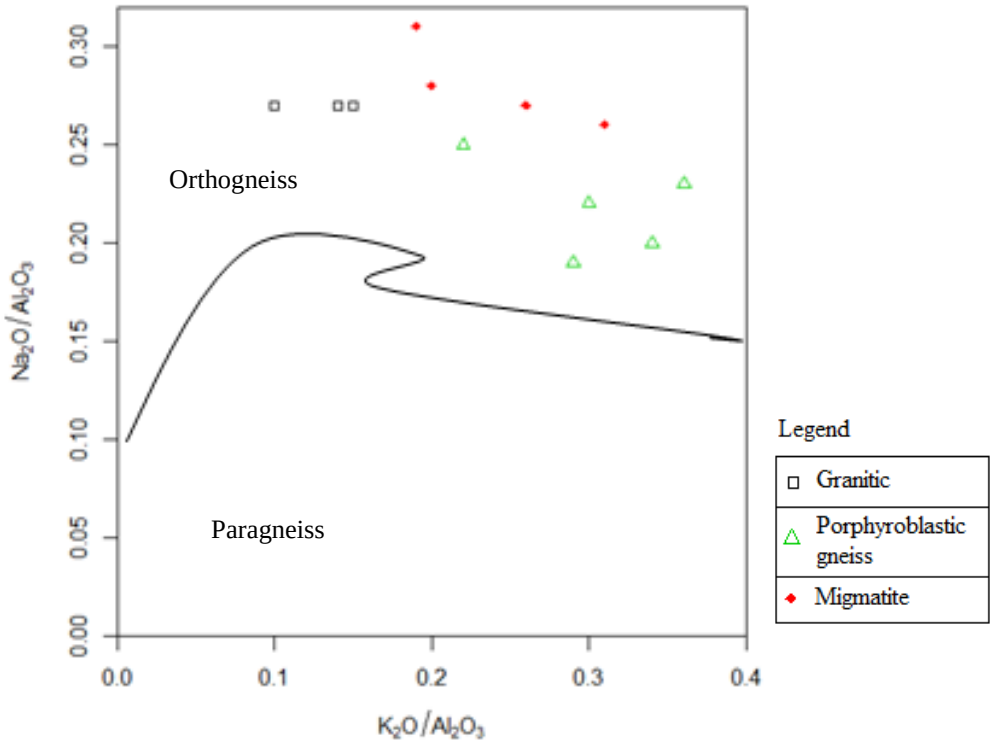

Figure 7: Igneous precursory was established in the plot of Na_2O/Al_2O_3 vs K_2O/Al_2O_3 after [18].

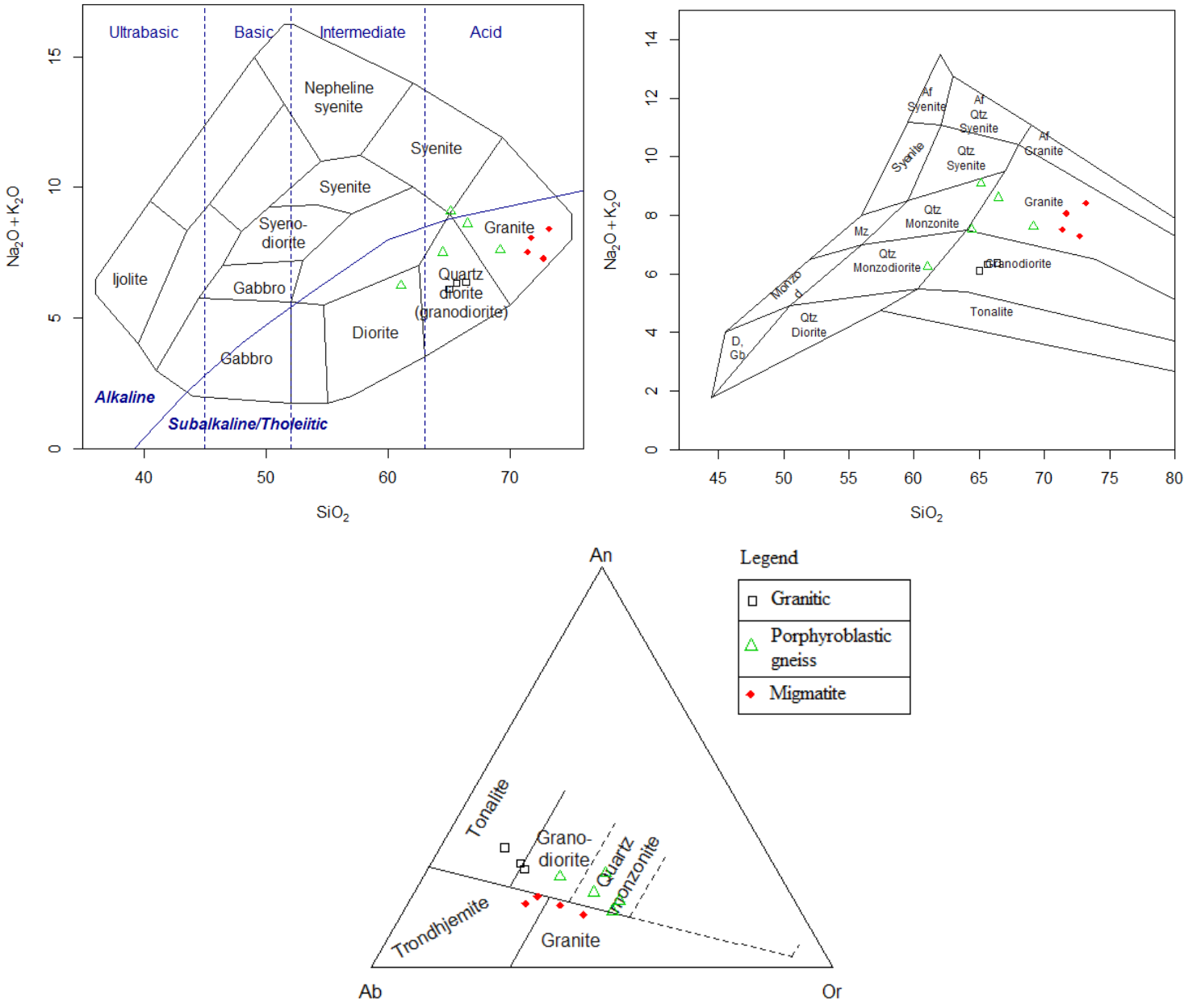

Figure 8: a) Total Alkali vs Silica plots of [19] and [20] revealed parentage of granitic to dioritic compositions for the migmatite complex of the study. b) Feldspar trilinear plot (Ab-An-Or) of [20] described the migmatite as Tonalite – Trondhjemite – Granodiorite (TTG).

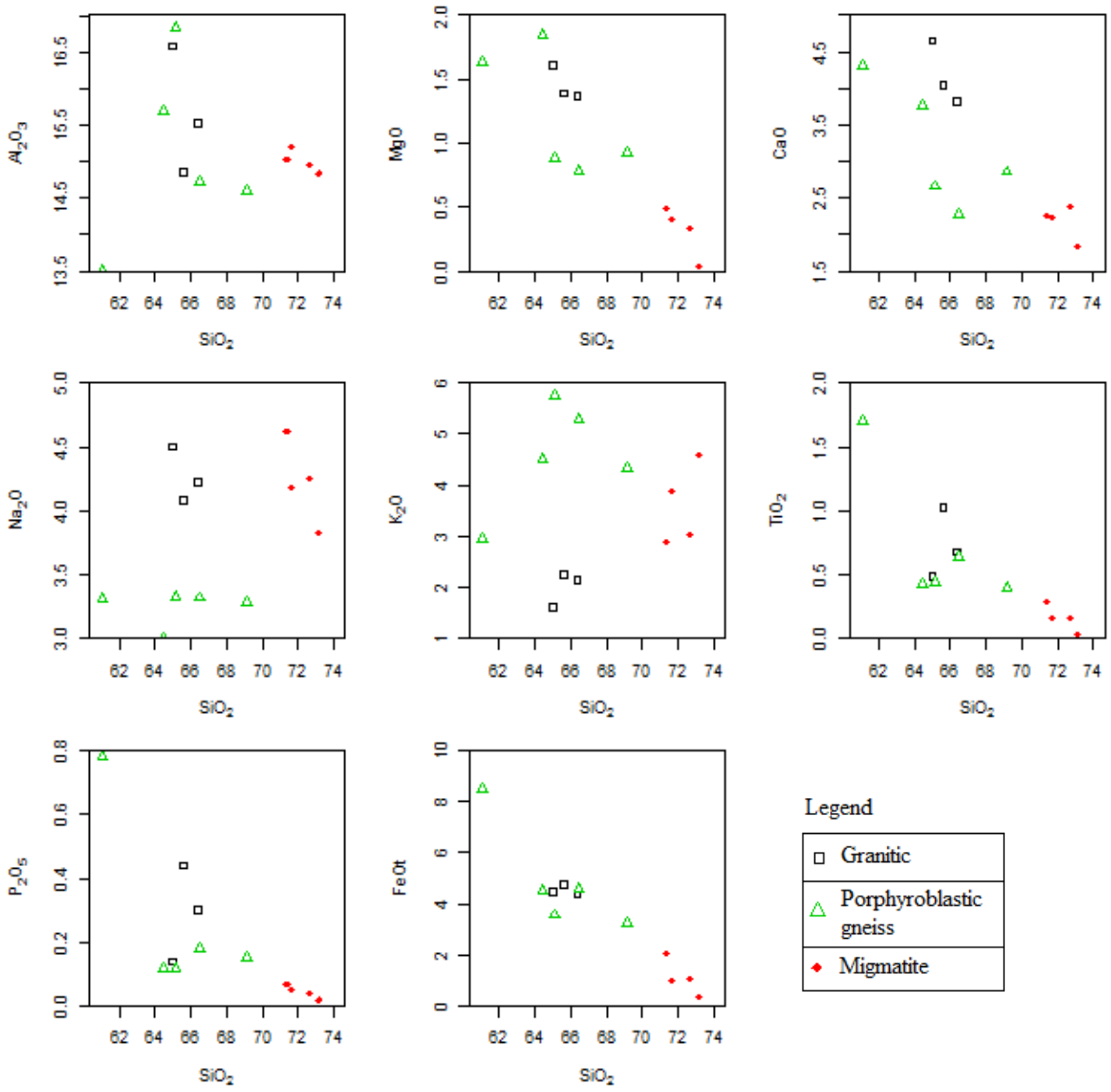

Figure 9: Bivariate plot of major oxide vs SiO_2 revealed correlation in oxides of FeOtot, MgO, CaO and TiO_2.

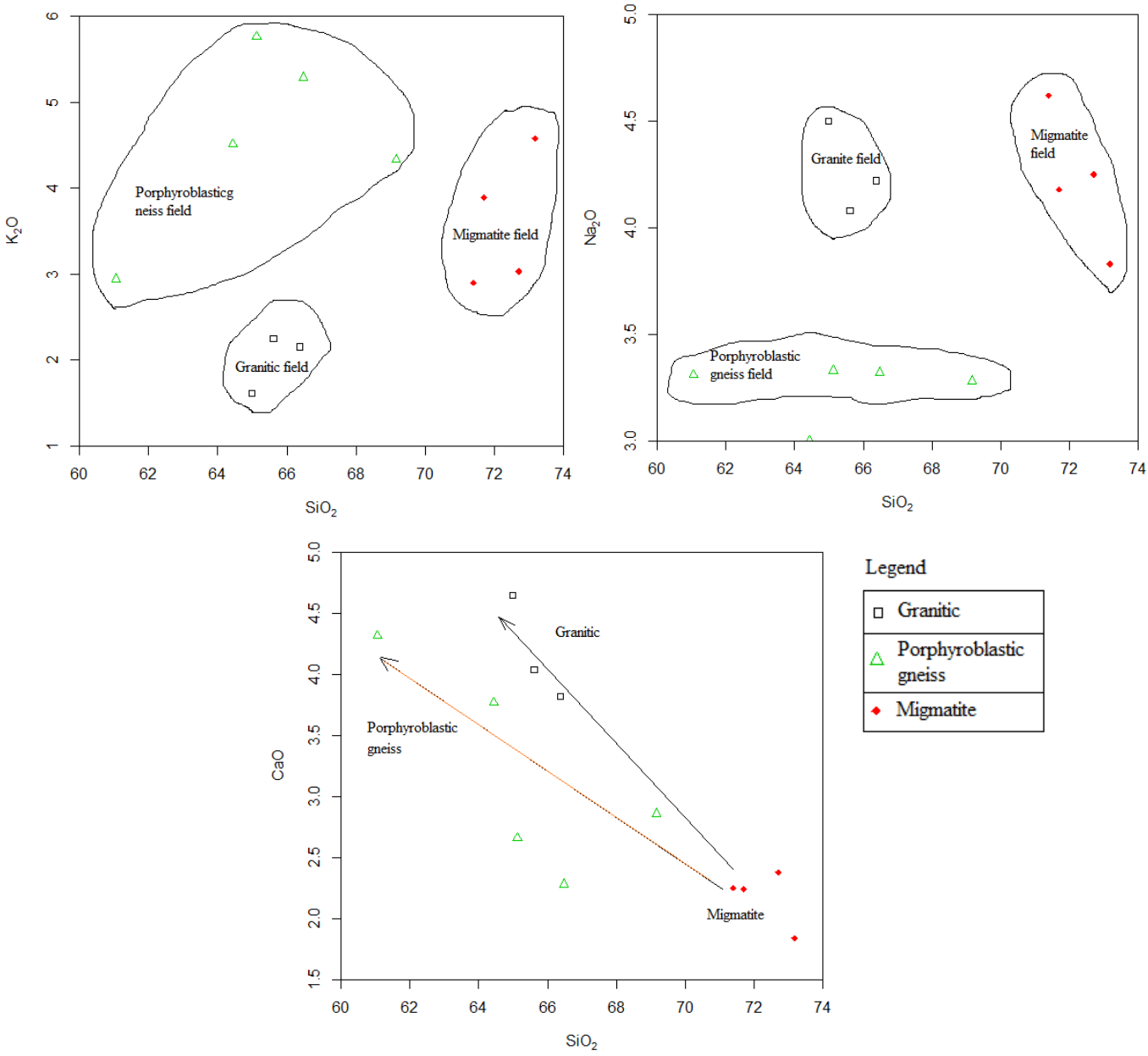

Figure 10: Plots of K_2O and Na_2O vs SiO_2 displayed discrimination of the migmatite. CaO vs SiO_2 revealed differential CaO enrichment during metamorphic differentiation associated with anatexis.

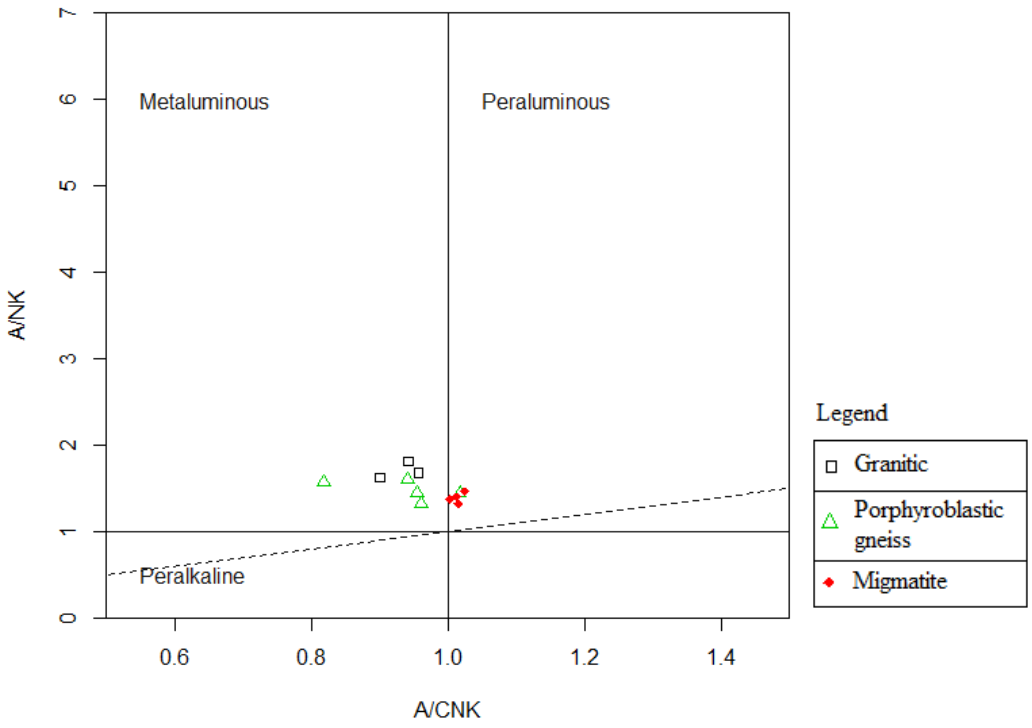

Figure 11: Plot of A/NK vs A/CNK of [22] illustrated peraluminous character for the migmatite and metaluminous character for the components.

(303.7 – 456.3) in the porphyroblastic gneiss with average Sr value at 371.02. The granitic component revealing the highest Sr value (686.1) corresponded to high values in CaO and norm An. Immobile high field strength elements (HFSE) revealed partitioning occurred during anatexis. Variable degrees of partial melting, ranging from moderate to high, must have been responsible for the enrichment of HFSE in the diatexite components. Respective average Zr and Hf values for the granitic and porphyroblastic gneiss were similar but higher than those observed for the migmatite component. Zr values ranging from 159.2 – 503.4 yielded average value of 329.53 for the granitic component while values ranged from 179 to 504.1 with average of 282.02 for the porphyroblastic gneiss. With average Zr value of 91.63, the migmatite showed the lowest values ranging from 34.6 – 149.2. Respective average Hf values for the granitic (7.77), porphyroblastic gneiss (7.62) and migmatite (2.45) components were observed for increase in order similar to Nb and Ta concentrations. Ba/Sr values revealed higher values in granitic component and migmatite relatively over the porphyroblastic gneiss with dictyonitic structure suggesting partial melting favours fractional melting of alkali feldspar and its partitioning in granitic melt. Higher normative albite over normative orthoclase for the granitic samples inferred that the alkali feldspars in the granitic melt are of albite compositions (Table 2). Thin section of the granitic compositions supports this claim (Fig. 5c and d). Relatively higher values in Rb/Sr and normative orthoclase inferred that the porphyroblastic gneiss has alkali feldspar composition as potassic feldspars. Plots of K_2O and Na_2O vs SiO_2 (Fig. 10) also supports this. Average Nb/Ta values were lower than 12 reported as the

Table 2: CIPW normative mineralogy for the migmatite components.

Sample Id	Q	C	Or	Ab	An	Di	Hy	Il	Hm	Tn	Ru	Ap
Gr1	21.09	0	9.51	38.08	20.29	0.34	3.85	0.15	4.95	1.01	0	0.33
Gr2	24.22	0.02	12.71	35.71	16.99	0	3.41	0.17	4.85	0	0.59	0.71
Gr3	24.13	0	13.3	34.52	15.56	0	3.46	0.17	5.26	1.13	0.48	1.04
OGB 01	21.48	0	31.26	28.09	9.67	0	1.94	0.15	5.12	0.33	0.43	0.43
OGB 02	21.72	0	17.37	28.01	13.29	0	4.09	0.41	9.46	2.14	0.61	1.85
OGB 03	17.05	0.58	34.04	28.18	12.41	0	2.19	0.13	3.96	0	0.37	0.28
OGB 04	19.64	0	26.65	25.39	16.05	0.56	4.35	0.17	5.05	0.81	0	0.28
OGB 05	26.62	0	25.59	27.75	12.3	0	2.32	0.17	3.62	0.64	0.05	0.36
Mgn1	28.08	0.36	17.14	39.09	10.71	0	1.22	0.06	2.26	0	0.26	0.17
Mgn2	29.44	0.28	27.07	32.41	9	0	0.1	0.01	0.4	0	0.02	0.05
Mgn3	27.24	0.17	22.99	35.37	10.79	0	1.02	0.04	1.12	0	0.14	0.12
Mgn4	30.91	0.46	17.91	35.96	11.55	0	0.85	0.02	1.22	0	0.15	0.09

average value for upper continental crust [23] in the granitic (7) and migmatite (5) samples suggesting influence of rock materials from middle or lower crust as possible protolith. The average Nb/Ta value for the porphyroblastic gneiss (14) was above the [22] value for upper continental crust.

4.3 Rare Earth Element Geochemistry

Rare earth element concentration (ppm) from components in the migmatite complex (Table 3a) and chondrite normalised values after [24] (Table 3b) showed enrichment in light rare earth elements (LREE). The REE normalised plot (Fig. 12) after [24] revealed an upper continental pattern with LREE enrichment for samples of the migmatite and its components. The migmatite samples showed least HREE concentrations with values closest to chondrite values while sample Mgn2 representing the migmatite plotted below chondrite values. Samples for the porphyritic gneiss and granitic components plotted closely and above the migmatite samples (Fig. 12). Eu anomalies were variable. Positive europium (Eu^{2+}) anomaly was revealed for the migmatite (schollen) samples while negative europium (Eu^{2+}) anomaly was observed for the relatively plagioclase-depleted porphyroblastic gneiss when compared with the granitic component. Samples of the granitic component did not show any form of Eu anomaly. This variation may be due to either biotite and or plagioclase fractionations or both.

Table 3a: Rare Earth Element (REE) concentration.

Sample Id	Gr1	Gr2	Gr3	OGB 01	OGB 02	OGB 03	OGB 04	OGB 05	Mgn1	Mgn2	Mgn3	Mgn4
La	29.1	81.9	138.8	94.3	127.9	84.5	48.2	60.0	25.6	2.3	12.6	13
Ce	54.3	160.2	279.2	187.9	271.2	155.4	95.8	129.7	48.4	3.3	21.2	25.2
Pr	5.73	17.91	31.82	19.05	29.18	16.10	9.97	13.41	4.97	0.26	2.24	2.49
Nd	20	66.3	122.9	66.3	104.7	53.0	34.9	47.0	17.3	0.8	7.5	8.5
Sm	3.2	10.69	17.74	9.85	17.85	7.34	6.11	8.70	2.51	0.17	1.18	1.21
Eu	0.89	2.6	4.39	1.85	2.23	1.34	1.13	1.21	0.63	0.54	0.5	0.58
Gd	2.59	7.66	11.87	6.08	11.78	4.08	4.66	6.92	1.87	0.22	1.06	0.86
Tb	0.35	1.05	1.59	1.03	1.97	0.67	0.82	1.27	0.18	0.02	0.14	0.11
Dy	1.94	5.27	7.79	5.05	10.10	3.16	4.14	6.68	0.81	0.12	0.64	0.55
Ho	0.31	0.91	1.5	0.94	1.97	0.63	0.89	1.20	0.14	0.03	0.13	0.09
Er	0.97	2.63	4.11	2.60	5.55	1.89	2.54	3.28	0.36	0.015	0.31	0.21
Tm	0.14	0.36	0.56	0.36	0.78	0.28	0.39	0.46	0.05	0.005	0.04	0.04
Yb	0.98	2.31	3.38	2.26	4.95	2.02	2.30	2.59	0.44	0.025	0.28	0.18
Lu	0.12	0.32	0.48	0.34	0.77	0.33	0.38	0.35	0.06	0.005	0.05	0.03

Table 3b: Normalised Rare Earth Element (REE) concentration after Boynton (1984).

REE	Gr1	Gr2	Gr3	OGB 01	OGB 02	OGB 03	OGB 04	OGB 05	Mgn1	Mgn2	Mgn3	Mgn4
LaN	93.87	264.19	447.74	304.19	412.58	272.58	155.48	193.55	82.58	7.42	40.65	41.94
CeN	67.20	198.27	345.54	232.55	335.64	192.33	118.56	160.52	59.90	4.08	26.24	31.19
PrN	46.97	146.80	260.82	156.15	239.18	131.97	81.72	109.92	40.74	2.13	18.36	20.41
NdN	33.33	110.50	204.83	110.50	174.50	88.33	58.17	78.33	28.83	1.33	12.50	14.17
SmN	16.41	54.82	90.97	50.51	91.54	37.64	31.33	44.62	12.87	0.87	6.05	6.21
EuN	12.11	35.37	59.73	25.17	30.34	18.23	15.37	16.46	8.57	7.35	6.80	7.89
GdN	10.00	29.58	45.83	23.47	45.48	15.75	17.99	26.72	7.22	0.85	4.09	3.32
TbN	7.38	22.15	33.54	21.73	41.56	14.14	17.30	26.79	3.80	0.42	2.95	2.32
DyN	6.02	16.37	24.19	15.68	31.37	9.81	12.86	20.75	2.52	0.37	1.99	1.71
HoN	4.32	12.67	20.89	13.09	27.44	8.77	12.40	16.71	1.95	0.42	1.81	1.25
ErN	4.62	12.52	19.57	12.38	26.43	9.00	12.10	15.62	1.71	0.07	1.48	1.00
TmN	4.32	11.11	17.28	11.11	24.07	8.64	12.04	14.20	1.54	0.15	1.23	1.23
YbN	4.69	11.05	16.17	10.81	23.68	9.67	11.00	12.39	2.11	0.12	1.34	0.86
LuN	3.73	9.94	14.91	10.56	23.91	10.25	11.80	10.87	1.86	0.16	1.55	0.93
Eu/Eu*	0.95	0.88	0.93	0.73	0.47	0.75	0.65	0.48	0.89	8.54	1.37	1.74
LaN/YbN	20.02	23.90	27.69	28.13	17.42	28.20	14.13	15.62	39.23	62.03	30.34	48.69
LaN/SmN	5.72	4.82	4.92	6.02	4.51	7.24	4.96	4.34	6.42	8.51	6.72	6.76
CeN/YbN	14.33	17.94	21.37	21.51	14.17	19.90	10.77	12.95	28.45	34.14	19.58	36.21
CeN/SmN	4.10	3.62	3.80	4.60	3.67	5.11	3.78	3.60	4.65	4.68	4.34	5.03
EuN/YbN	2.58	3.20	3.69	2.33	1.28	1.89	1.40	1.33	4.07	61.42	5.08	9.16
Sum REE	120.62	360.11	626.13	397.91	590.93	330.74	212.23	282.77	103.32	7.81	47.87	53.05

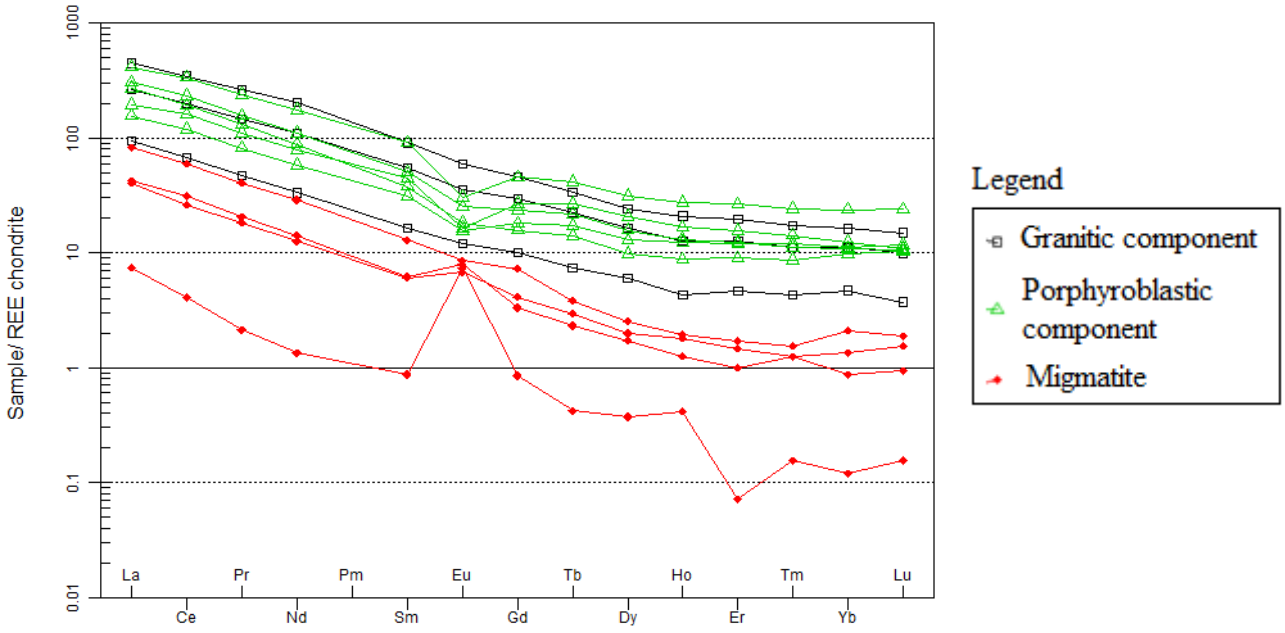

Figure 12: Rare earth element plot normalised after [24] revealed variable fractionation for Eu.

4.4 Metamorphic facies

Mineral composition of quartz, plagioclase, microcline, biotite, hornblende, garnet, zircon and muscovite suggest metamorphic grade from lower greenschist to upper amphibolite facies. The absence of pyroxene and sillimanite in the components studied and evidence from petrological modelling of migmatite [25] suggest that temperatures during anatexis did not exceed 880^{o}C. Figure 13 illustrated samples of the gneiss (migmatite and porphyroblastic gneiss) plotted along the anorthite – Almandine line. Spider plot normalised after [23] (Fig. 14) showed that the samples from the migmatite with schollen structure representing the diatexite had lesser amounts of incompatible elements when compared with the metatexite components, the granitic and the porphyroblastic gneiss parts. Sr enrichment implying plagioclase fractionation is widespread, though with slight variations, in all parts of the migmatite as all samples tend to cluster. The migmatite and the porphyroblastic gneiss are enriched relatively over the granitic components in potassium (K) suggesting relative abundance in K rich minerals such as alkali feldspar and biotite. Anatexis may have played an appreciable role in the partitioning of more immobile high field strength (HFS) elements as the migmatite samples partitioned closer to chondrite normalised values than the other components.

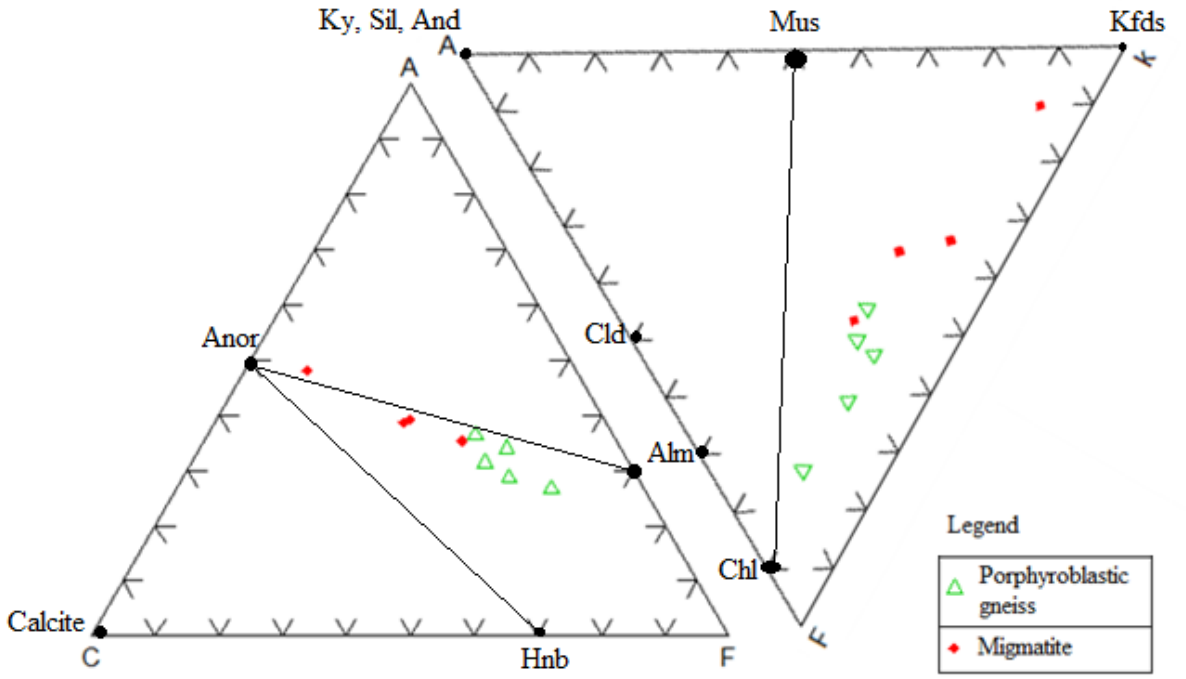

Figure 13: ACF and AKF plot for samples of the migmatite display upper amphibolite facies.

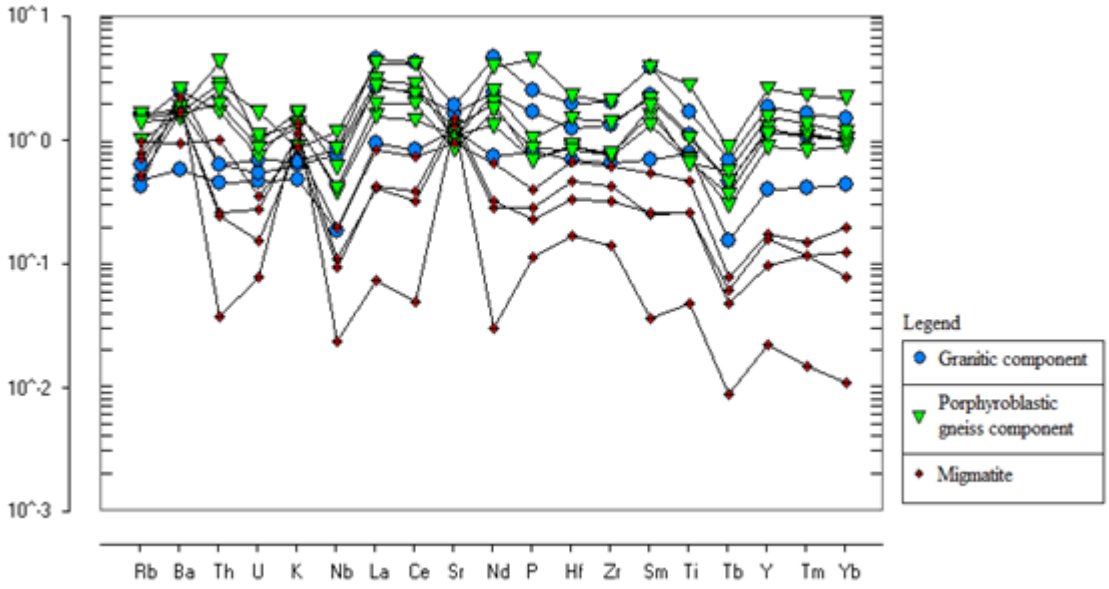

Figure 14: Spider plot of trace elements normalised after Upper Continental Crust values of [23] revealed variable fractionation of high field strength elements, Zr, Hf, Nb, Th and HREE.

5. Conclusion

The migmatite complex of southwestern Nigeria displayed several structural varieties such as stromatic, dictyonitic, schollen, surreitic migmatite gneisses. Field evidences showed that the stromatic and the dictyonitic components representing metatexite were closely related to quartzite ridges lying unconformably on the migmatite complex. The schollen migmatite typifying the diatexite were notably observed to be exposed at places farther from quartzite exposures. Major oxide geochemistry showed that the granitic components are tonalitic to granodioritic with enrichment in CaO and MgO. The porphyroblastic gneiss is granodioritic to quartz monzonitic while the migmatite is trondhjemite to granitic. These compositions describe the Tonalite-Trondhjemite-Granodiorite (TTG) character of the migmatite gneiss complex. Bivariate plot of K_2O and Na_2O vs SiO_2 inferred differential partitioning during anatexis. The granitic component showed enrichment in Na_2O while the porphyroblastic gneiss showed enrichment in K_2O. Normative albite was higher in the granite while normative orthoclase was higher in the porphyroblastic gneiss. The migmatite with schollen structure and the granitic component representing the diatexite parts revealed relatively higher Rb/Sr and lower Nb/Ta values than the porphyroblastic gneiss representing the metatexite. The migmatite samples with higher silica values plotted closest to chondrite values in the REE plot. This may infer having components representing primitive precursors mixed with more evolved components such as the leucosome of granitic compositions.

References

[1] Rahaman, M. A., 1976. Review of the basement geology of southwestern Nigeria. In: C. A. Kogbe (ed), Geology of Nigeria. Elizabethan Publ. Co. Lagos, Nigeria. pp 41–58.

[2] Nedelec, A. and Bouchez, J., 2015. Granite: Petrology, Structure, Geological setting and Metallogeny. Oxford University Press. 335p.

[3] Patino Douce, A. E., 1999. What do experiments tell us about the relative contributions of crust and mantle to the origin of granitic magmas? In: Castro, A., Fernandez, C. and Vignerisse, J. L. (eds) Understanding Granites: Integrating New and Classical Techniques. Geological Society, London, Special Publications, pp. 168, 55-75.

[4] Turtle, O. F. and Bowen, N. L., 1958. Origin of granite in the light of experimental studies in the $NaAlSi_3O_8$- $KAlSi_3O_8$- SiO_2-H_2O, Geological Society of America Memoirs, No. 74, 153p.

[5] Milord, I., Sawyer, E. W. and Brown, M., 2001. Formation of diatexite migmatite and granite magma during anatexis of semi-pelitic metasedimentary rocks: an example from St. Malo, France. Journal of Petrology. Vol. 42 (3), pp. 487–505.

[6] Zeng, L. Saleeby, J. B. and Ducea, M., 2005. Geochemical characteristics of crustal anatexis during the formation of migmatite at the Southern Sierra Nevada, California. Contib. Mineral Petrol. Springer-Verlag. 150 (4), pp. 386–402.

[7] Sawyer, E. W., 1998. Formation and evolution of granitic magmas during crustal reworking: the significance of diatexite. Journal of Petrology **39**, pp. 1147-1167.

[8] Mehnert, K. R., 1968. Migmatites and the origin of Granitic rocks. Elsevier. Amsterdam.

[9] Oyawoye, M. O. 1964. The Geology of the Nigerian Basement Complex. Journ. Nigerian Min. Geol. And Metall. Soc. Vol. 1., pp 87–102.

[10] Rahaman, M. A., 1976. Review of the Basement Geology of the South-Western Nigeria. In: C. A. Kogbe (ed), Geology of Nigeria. Elizabeth Publ. Co. Lagos, Nigeria. pp 41–58.

[11] Afolabi, O. A., Kolawole, L. L., Abimbola, A. F., Olatunji, A. S. and Ajibade, O. M., 2013. Preliminary study of the geology and structural trends of the lower Proterozoic Basment rocks in Ogbomoso, SW Nigeria. Jour. of Environment and Earth Science, Vol 3, No. 8, pp. 82–95.

[12] Okezie, L. N., 1974. Geological Map of Nigeria, Scale 1:2,000,000.- Geological Survey; Lagos.

[13] Key, R. M., 1992. An introduction to the crystalline basement of Africa.- In: Hydrogeology of crystalline basement aquifers in Africa, E. P. Wright & W.G. Burgess (eds.), Geol. Soc. Spec. Publ. London 66, pp. 29-57.

[14] Oluyide, P. O., Nwajide, C, S. and Oni, A. O., 1998. The Geology of Ilorin area. Ministry of Solid Minerals Development, Geol. Surv. of Nig. Bulletin No. 42, 84P.

[15] Jones, H. A. and Hockey, R. D., 1964. The Geology of Part of South-western Nigeria. Geological Survey of Nigeria, Bull. No 31. 101p.

[16] Sawyer, E. W., 2008b. Working with Migmatite. In E. W. Sawyer and M. Brown (eds). Working with Migmatite. Mineralogical Association of Canada, Short Course Series Vol. 38, Quebec City, Quebec, pp 1–28.

[17] Nabelek, P.I. (1997) Quartz-sillimanite leucosomes in high-grade schists, Black Hills, South Dakota: A perspective on the mobility of Al in high-grade metamorphic rocks. Geology, 25, 995–998.

[18] Garrels, R. M. and MacKenzie, F. T., 1971. Evolution of Sedimentary rocks. Norton & Co. New York. 394P.

[19] Cox, K. G., Bell, J. D. & Pankhurst, R. J., 1979. The Interpretation of Igneous Rocks. George Allen & Unwin.

[20] Middlemost, E. A. K., 1985). Naming materials in the magma-igneous rock system. Earth-Sciences Reviews 37, pp. 215–224.

[21] O'Connor, J. T., 1965. A classification for quartz-rich igneous rocks based on feldspar ratios. In: US Geological Survey Professional Paper **B525.** USGS, pp. 79–84.

[22] Shand, S. J., 1943. Eruptive Rocks. Their Genesis, Composition, Classification, and Their Relation to Ore-Deposits with a Chapter on Meteorite. , 2nd edn New York: John Wiley & Sons. 444 P.

[23] Taylor, S. R. and McLennan, S. M., 1985. The Continental crust: Its Composition and Evolution. Oxford: Blackwell, 312p.

[24] Boynton, W. V. 1984. Cosmochemistry of the rare earth elements: meteorite studies. In: Henderson P (eds) Rare Earth Element Geochemistry. Elsevier, Amsterdam, pp 63-114.

[25] White, R. W., 2008b. Insights gained from the petrological modeling of Migmatites: particular reference to mineral assemblages and Common replacement textures. In E. W. Sawyer and M. Brown (eds). Working with Migmatite. Mineralogical Association of Canada, Short Course Series Vol. 38, Quebec City, Quebec, pp. 77-96.